

OPTICAL VARIABILITY IN IBL S5 0716+714 DURING THE 2013–2015 OUTBURSTS

NAVPREET KAUR ¹, KIRAN S. BALIYAN, S. CHANDRA ², SAMEER ³, S. GANESH
Astronomy & Astrophysics Division, Physical Research Laboratory, Ahmedabad 380009, India
(Dated: Under Review in AJ)
Draft version May 15, 2018

ABSTRACT

With an aim to explore optical variability at diverse timescales in BL Lac source S5 0716+714, it was observed for 46 nights during 2013 January 14 to 2015 June 01 when it underwent two major outbursts. The observations were made using the 1.2-m Mount Abu InfraRed Observatory telescope mounted with a CCD camera. On 29 nights, the source was monitored for more than two hours, resulting in 6256 data points in R-band, to check for the intra-night variability. Observations in B, V and I bands with 159, 214, and 177 data points, respectively, along with daily averaged R-band data are used to address inter-night and long-term variability and the color behavior of S5 0716+71. The study suggests that the source shows significant intra-night variability with a duty cycle of more than 31% and night-to-night variations. The average brightness magnitudes in B, V, R & I bands were found to be 14.42(0.02), 14.02(0.01), 13.22(0.01) & 13.02(0.03), respectively, while S5 0716+714 was historically brightest with $R = 11.68$ mag on 2015 January 18, indicating that source was in relatively high state during this period. A mild bluer when brighter behavior, typical of BL Lacs, supports the shock-in-jet model. We notice larger amplitudes of variation when the source was relatively brighter. Based on the shortest time scale of variability and causality argument, upper bound on the size of the emission region is estimated to be 9.32×10^{14} cm and the mass of the black hole to be $5.6 \times 10^8 M_{\odot}$.
Subject headings: galaxies: active — BL Lacertae objects: general— BL Lacertae: individual (S5 0716+714) — method: observational—technique: photometry.

1. INTRODUCTION

Blazars are a sub-class of active galactic nuclei (AGN) with their relativistic jet oriented towards the observer's line of sight (Blandford & Königl 1979; Urry & Padovani 1995) leading to the Doppler boosted emission from the jet. They show extreme variability in their brightness and polarization over the time scale of minutes to tens of years. Owing to these properties, their study serves as a tool to probe deeper into the central engine to understand the structure and emission processes in AGN. The continuum spectral energy distribution (SED) of blazars is dominated by the non-thermal emission with two broad peaks covering entire electromagnetic spectrum (EMS), ranging from radio to high energy γ -rays. The first peak in the SED lies in the sub-mm to X-ray region and is known to be due to synchrotron process in which the relativistic electrons gyrate in a strong magnetic field present inside the jet (Urry & Mushotzky 1982) and radiate by cooling. The second, high energy peak, is understood to be due to inverse Compton scattering of low energy photons, the origin of which is not understood well. Under the leptonic scenario (see, Böttcher 2007, for a review), inverse Compton scattering of the low energy photons by the relativistic electrons, which gave rise to the synchrotron emission, is responsible for the high energy peak. The seed photons which are up-scattered, could either be synchrotron photons (Self Synchrotron Compton; SSC) or external photons from the accretion

disk, the broad-line region, molecular torus, cosmic microwave background etc. (external Compton; EC), or a combination of both (Maraschi et al. 1994, and references there-in). The exact source of these seed photons is still an open question. As an alternative approach, hadronic models (Mannheim & Biermann 1989) are also used to explain the high energy component in the SED (Zdziarski & Böttcher 2015).

Blazars consist of flat spectrum radio quasars (FSRQ) and BL Lac objects, with FSRQs differentiated from BL Lacs by the presence of broad emission lines in their spectrum (with equivalent width, $EW > 5 \text{ \AA}$; (Urry & Padovani 1995; Laurent-Muehleisen et al. 1999)). Depending upon the frequency of the synchrotron peak in their SED, BL Lacs are further classified into three categories (Abdo et al. 2010) - low, intermediate and high energy peaked BL-Lacs, abbreviated as LBL, IBL and HBL, respectively. The synchrotron peak frequency, ν_{sync}^p for LBL lies below 10^{14} Hz; for IBL, between 10^{14} Hz and 10^{15} Hz; while for HBL $\nu_{sync}^p > 10^{15}$ Hz. Fossati et al. (1998) found an anti-correlation between the synchrotron peak frequency and the synchrotron peak luminosity in the blazar. Also, the Compton dominance parameter, which is the ratio of inverse Compton peak luminosity to the synchrotron peak luminosity, decreases from the high-luminosity (FSRQs) to low-luminosity blazars (BL-Lacs). This could be due to the presence of external seed photons, from BLR or torus, leading to higher inverse-Compton luminosity (Sikora et al. 1994). It was, therefore, noticed that the luminosity, degree of polarization and the γ - ray dominance decrease from FSRQ to LBL, IBL, and HBL while ratio of non-thermal to thermal component and the synchrotron peak frequency

¹ Indian Institute of Technology, Gandhinagar, Ahmedabad 382355, India; E-mail: navpreet@prl.res.in

² North-West University, Potchefstroom 2520, South Africa

³ Department of Astronomy & Astrophysics, Davey Laboratory, Pennsylvania State University, PA 16802

increase, indicating a blazar sequence (Maraschi et al. 1994; Fossati et al. 1998; Ghisellini & Tavecchio 2009).

Since AGN are not resolvable by any existing telescope facility, understanding their structure and emission mechanisms pose a big challenge. Blazars, which are variable over diverse time-scales across the whole spectrum, provide a viable tool as their variability time-scales, correlated variations among multi-frequency light-curves, color variations and SEDs are used as probes (Marscher 2008; Marscher et al. 2010; Jorstad et al. 2010; Dai et al. 2015; Ciprini et al. 2007, and references there-in). The temporal variability in blazars has been classified into three categories, namely, long-term variability (LTV) - months to years (Fan 2005; Fan et al. 2009), short-term variability (STV) - a few days to months, and intra-night variability (INV) or micro-variability - a few minutes to several hours within a night (Wagner & Witzel 1995; Kaur et al. 2017b). Though the mechanisms responsible for the variability remain largely unclear, long-term variability could be due to the disk perturbation/instability or structural changes in the jet, e.g., precession, bending of jet (Marscher & Gear 1985; Kawaguchi et al. 1998; Nottale 1986; Nair et al. 2005). The STV in optical flux, including inter-night variability, could be caused by intrinsic and extrinsic processes, e.g., injection of fresh plasma in the jet, shock moving down the turbulent jet, changes in the boosting factor due to change in the viewing angle, gravitational micro-lensing etc, and sometimes results in the spectral changes (Ghisellini et al. 1997; Villata et al. 2002; Hong et al. 2017). The INV, also known as microvariability, could be due to shock compression of the plasma in the jet, shock interacting with local inhomogeneities, blob passing through quasi-stationary core, changes in the viewing angle in a jet-in-jet scenario (Narayan & Piran 2012) or other processes causing small scale jet turbulence (Marscher & Gear 1985; Marscher 2008; Chandra et al. 2011; Kaur et al. 2017b). However, the exact processes responsible for variability, in particular INV, are not well understood and significant amount of work is required to have a better understanding of this complex phenomenon.

The intermediate BL Lac object S5 0716+714 is one of the most active blazars and makes a perfect candidate for variability study on the blazars at diverse time scales (Aliu et al. 2012). It is available in the sky for a longer time during the night (due to its high declination), is almost always active, fairly bright, and hence can be observed with moderate facilities. It was discovered by Kuehr et al. (1981) in NRAO 5 GHz radio survey with flux larger than 1 Jy^4 and due to its featureless spectra (Biermann et al. 1981), was categorized as a BL-Lac source. Nilsson et al. (2008) derived a redshift of 0.31 ± 0.08 by taking the host galaxy as a standard candle, but recently Danforth et al. (2013) put a statistical upper limit of $z < 0.322$ (with 99% confidence) on its redshift. The source S5 0716+714 has been observed across the EMS, including its discovery as a TeV candidate in 2008 by MAGIC collaboration (Anderhub et al. 2009), when a strong optical and γ -ray correlated activity was noticed.

S5 0716+714 shows high duty cycle of variation (DCV)

as reported by Chandra et al. (2011, and references there-in). Due to all these properties, it has been the target of several multi-wavelength campaigns around the globe (Wagner & Witzel 1995; Villata et al. 2002; Raiteri et al. 2005; Nesci et al. 2005; Montagnani et al. 2006; Gupta et al. 2008; Dai et al. 2015), focusing on INV and STV. After being reported in its high phase, the object was followed by Bachev et al. (2012) who claimed historical maxima and minima of 12.08 (MJD 56194) and 13.32 (MJD 56195) in R-band, respectively. Rani et al. (2013) found the γ -ray emission to be correlated with optical and radio, supporting SSC mechanism responsible for the high energy emission. However, an orphan flare in X-rays indicated to the limitation of such simple scenario.

Investigating the long-term variability trend, Nesci et al. (2005, and references there-in) reported a decreasing average brightness of the source during 1961-1983 followed by an increasing one upto 2003, superposed with short term flares. They extracted source brightness data from photographic plates obtained from the Asiago Observatory, POSS1 and Quick V surveys dating back to 1953 to generate long-term light curves. It underlined the importance of the astronomical data, even if taken for some other purpose. Based on these data, they even predicted a decrease in the mean brightness of the source during the next 10 years, i.e., after 2003. Indeed, the source was inferred, from the 2003 to 2014 optical data, to be in decreasing brightness phase by Chandra (2013); Baliyan et al. (2016) and the present work, suggesting a precessing jet with increasing viewing angle.

The blazar S5 0716+714 has undergone several optical outbursts in the past, superposed on the mean decreasing or increasing long-term trends as reported by many workers (Raiteri et al. 2003; Nesci et al. 2005; Gupta et al. 2008; Larionov et al. 2013). Micro variability (INV) on the time-scales of a few hours to 15 minutes is reported (Chandra et al. 2011; Rani et al. 2013; Man et al. 2016, and references there-in) with S5 0716+714 showing bluer-when brighter (BWB) behaviour in general. On the other hand, Raiteri et al. (2003) found a weak correlation with color, while others did not find any correlation between color and brightness (Stalin et al. 2009; Agarwal et al. 2016; Wu et al. 2005). The blazar S5 0716+714 has also been reported to show (quasi-) periodic variations (QPV) in optical at several epochs and at many time scales ranging from sub-hours to years (Raiteri et al. 2003; Gupta et al. 2008). However, Bhatta et al. (2016) did not find 3 and 5 hr QPV as genuine. Recently, Hong et al. (2018) reported 50 min QPV when the source was relatively fainter during 2005 - 2012, ascribing it to the activity in the innermost orbit of the accretion disk.

The blazar S5 0716+714 was reported achieving new historical brightness levels (11.68 in R-band) in optical on 2015 January 18 by Chandra et al. (2015a,b), reassuring that it will never stop to surprise us. It, therefore, justifies a continuous coverage of the source to help us understand the nature of blazars in general and S5 0716+714 in particular. Keeping this objective in mind and to understand the variability characteristics, chromatic behaviour and relationship between variability amplitude and brightness of the source, here we present our results obtained from the observations during January, 2013 to June, 2015. Section 2 describes the observations

⁴ $1 \text{ Jy} = 10^{-23} \text{ erg cm}^{-2} \text{ s}^{-1} \text{ Hz}^{-1}$

and data analysis; section 3 presents the results and discussions while section 4 summarizes the work.

2. OBSERVATIONS AND DATA REDUCTION/ANALYSIS

To investigate intra-night and inter-night variability in BL-Lac source S5 0716+714, we carried out optical observations using the 1.2m telescope of the Mount Abu Infrared Observatory(MIRO), operated by the Physical Research Laboratory, Ahmedabad. The observatory is located at Gurushikhar mountain peak, about 1680 m above the sea-level, in Mount Abu (Rajasthan), India, with a typical seeing of 1.2 arcsec. The observations were taken with liquid-nitrogen cooled Pixcellent CCD camera as the backend instrument, equipped with Johnson-Cousins optical BVRI filter set. The dimension of the CCD array is 1296 x 1152 pixels of size 22 μm each. The field of view (FOV) is about 6.5 x 5.5 arcmin² with a plate scale of 0.29 arcsec/pixel. The CCD readout time is 13 seconds with readout noise of four electrons and negligible dark current when cooled to a temperature of about -120°.

In order to study INV (microvariability), as a strategy, we monitored the source for a minimum of two hours in the Johnsons R-band with a high temporal resolution (less than a minute) to resolve any rapid flare, while for STV and LTV in the source brightness and color, 4/5 images were taken in B, V and I-bands everyday during the campaign period. The source and its comparison/control stars, as they appear in the finding chart available at the web-page of the Heidelberg University⁵, – having brightness close to that of the source (Howell & Jacoby 1986) were kept in the same observed frame. Differential photometry was performed to minimize the effect of non-photometric conditions (however, majority of the observations were made during photometric nights), like minor fluctuations due to turbulent sky and other seeing effects. The exposure time was decided by keeping the counts well below the saturation limit and in the linear regime of our CCD (Cellone et al. 2000a). Several twilight flat field images and bias images were taken on each observation night to calibrate the science images. By following the above mentioned strategy, a total of 6256, 159, 214 and 177 images in R, B, V and I-band, respectively, were obtained and subjected to analysis.

The observed data were checked for spurious features, if any, and reduced using IRAF⁶ standard tasks- bias subtraction, flat fielding, cosmic ray treatment etc. The comparison stars 5 and 6⁷, present in the source field were chosen to perform differential photometry. Other stars (stars 2 and 3) in the field were too bright to be used for differential photometry as they could introduce errors (from differential photon statistics and random noise, like sky) (Howell et al. 1988). An optimum aperture size, three times the FWHM, was used based on the prescription by Cellone et al. (2000a), as a smaller apertures can give better Signal-to-Noise(SNR), but might lead to

spurious variations if the seeing was not good, while a larger aperture would have significant contribution from the host galaxy thermal emission(Cellone et al. 2000b) and might suppress the genuine variations in the blazar flux. Aperture photometry on the blazar S5 0716+714 and comparison stars 5 & 6, using the same aperture size, was performed using DAOPHOT package in IRAF on photometric nights.

The aperture photometry technique was employed on a total of 6806 images in BVRI-bands and the source magnitudes were calibrated with the average magnitude of the comparison stars 5 and 6, which were also used to check for the stability of sky during observations, as described in equation 1 and equation 2. No correction for host galaxy of S5 0716+714 was applied as the host galaxy is much fainter with R-band >20 mag (Montagnoli et al. 2006) than the central bright source. The differential light curves (LCs) were constructed to detect INV, while BVI & R band long-term LCs were generated from daily averaged values in each band. To quantify the INV nights, we applied several statistical tests, for example confidence parameter test (C-test), amplitude of variability (A_{var}) test, as discussed in the next section.

3. RESULTS AND DISCUSSION

As already mentioned earlier, the photometric data obtained after the aperture photometry were used to plot the intra-night and inter-night light curves. Though the lightcurves themselves are not sufficient to reveal the complexities of the variability and blazar phenomena, they are good indicators of the emission mechanism and can help put constraints on various models. The nature of most of the light curves differs from one night to the other, indicating to the emission from random and turbulent process in the jet. Since the physical mechanisms which trigger blazar variability, especially on intra-night time scales, are still debatable, any detailed study of LCs should add to our understanding.

In order to identify and characterize the nights showing INV, we performed variability amplitude and confidence parameter (C-test) tests. In the following we also discuss STV, LTV and color behaviour of the source during the period of our observing campaign.

3.1. Intra-night variability

Blazars show rapid variability which can sample very compact sizes of their emission regions. To determine the number of INV nights, we first excluded the not-photometric nights when sky conditions were changing drastically, and those with less than two hours of monitoring. We were left with 29 nights that qualified this criterion during 2013 January - 2015 June. The LCs for S5 0716+714, being very complex with a number of features, made it very difficult to infer INV from just visual inspection, barring a few clear cases. To resolve this problem, following statistical methods are used to quantify the INV.

Confidence parameter test (C-test): The C-test was first introduced by Jang & Miller (1997) and further generalized by Romero et al. (1999). It is basically a ratio between calibrated source magnitudes and the differential magnitude of the comparison stars, given as,

⁵ <http://www.lsw.uni-heidelberg.de/projects/extragalactic/charts/0716+714.html>

⁶ IRAF-Image Reduction and Analysis Facility is data reduction and analysis package by NOAO, Tucson, Arizona operated by AURA, under agreement with NSF.

⁷ Stars taken from the sequence A,B,C,D by Ghisellini et al. (1997) and corresponding sequence, 2, 3, 5, 6 by Villata et al. (1998)

$$C = \frac{\sigma_{S-C_{5,6}}}{\sigma_{C6-C5}} \quad (1)$$

where, $C_{5,6}$ is the average of difference in instrumental and standard magnitudes of stars 5 and 6, $\sigma_{S-C_{5,6}}$ and σ_{C6-C5} are the standard deviations of differential LCs. We consider the source to be variable when confidence parameter is greater than 2.57 (i.e., $C > 2.57$) for more than 3σ confidence (or 99 % confidence level)(Jang & Miller 1997). The standard deviation σ for differential light curves is given by,

$$\sigma = \sqrt{\frac{\sum (m_i - \bar{m})^2}{N - 1}} \quad (2)$$

where, $m_i = (m_2 - m_1)_i$ is the differential magnitude of the two objects, $\bar{m} = \frac{m_2 - m_1}{N}$ represents differential magnitude averaged over the night and N is the total number of data points.

F-test: F-test, also known as Fisher-Snedecor distribution test, measures the sample variances of two quantities i.e, variance of calibrated source magnitudes and that of the differential magnitudes of the comparison stars. To test the significance of variability during each night, it is written as,

$$F = \frac{\sigma_B^2}{\sigma_{CC}^2} \quad (3)$$

where σ_B^2 , σ_{CC}^2 are the variances in the blazar magnitudes and differential magnitudes of the standard stars for nightly observations, respectively. An F-value of ≥ 3 implies variability with a significance of more than 90% while an F-value of ≥ 5 corresponds to 99% significance level.

Amplitude of variability (A_{var}): The intra-night amplitude of variability in the source is calculated by using the expression given by Heidt & Wagner (1996),

$$A_{var} = \sqrt{(A_{max} - A_{min})^2 - 2\sigma^2} \quad (4)$$

where, A_{max} and A_{min} are the maximum and minimum magnitudes in the intra-night calibrated light curve of the source and σ is the standard deviation in the measurement. For a night to be considered as variable, A_{var} should be more than 5%.

3.1.1. INV light curves and duty cycle of variation (DCV)

After performing statistical tests on the entire data set, we get 9 out of a total of 29 nights which are found to be variable based on all the above mentioned criteria i.e., $C \geq 2.57$, $F \geq 5$ for more than 99% confidence level and $A_{var} \geq 0.05$ mag. Figure 1 shows the light curves for these INV nights where time in Modified Julian Date (MJD) is plotted along X-axis and the brightness magnitude in R-band along Y-axis. Lower curve is the differential LC for the two comparisons (5 and 6), to check the stability of that particular night, thus providing extent of uncertainty in the source values. The *rms* values of these differential lightcurves for comparison stars are a measure of accuracy in our magnitude measurements.

Upper curve (solid circles) shows the calibrated brightness magnitudes for the source. The plotted photometric errors are of the order of a few milli-magnitudes.

The INV light-curves (Figure 1) feature monotonic rise or fall, slow rise or decay with rapid fluctuations superimposed on them, alongwith a few LCs indicating to a possibility of quasi-periodic oscillations with short timescale. It can be noted that the shapes of most of the nightly lightcurves are different, as also reported by several other authors (Chandra et al. 2011; Kaur et al. 2017b; Hong et al. 2018, and references there-in) indicating that the emission processes are stochastic and complex in nature. A symmetric flare in a lightcurve would mean the cooling timescale is much shorter than the light-crossing timescale. On the night of 2013 February 12 (Fig. 1), the brightness decays slowly with no distinct peak, with total change in the amplitude of variation by about 7.5%. In the same figure, a slow increase in flux by about 0.07 mag in about 2.6 hr, with several rapid fluctuations superimposed (including one with 0.04 mag in about 30 min) is noticed on 2013 March 6. Next day LC starts with slight decreasing trend but begins brightening up at MJD 56358.88, with a rapid increase after 1.44 hr leading to 0.06 mag ($>2\sigma$). The flux decreases up to MJD 56607.0 and then remains stable within errors on 2013 November 11. The INV LC on 2013 March 12 shows interesting features with a brightening by 0.11 mag in about 30 min, followed by a decay of about 0.17 mag in about one hour. It starts increasing again reaching initial level of about 13.41 mag. A slow decrease in flux and then relatively faster increase by about 0.07 mag within about 70 min characterizes the LC on 2013 December 28(Fig. 1). A significant increase in flux by 0.13 mag within about 2.9 hr is noticed on 2013 December 30, while on 2014 December 02 night, brightness decreases continuously, with no peak. On 2014 December 3, flux rises by 0.08 mag within 2.4 hr during the total monitoring time of about 6 hrs.

However, it is difficult to determine variability time scales accurately only from visual inspection of LCs and therefore, in the next section we introduce and use structure functions and later analyze them to estimate required parameters.

Duty Cycle of variation: Most of the blazars show very high probability of variation even on intra-night time scales with an amplitude of variation of a few tenths of magnitude, for example, CTA 102: Bachev et al. (2017), 3C 66A: Kaur et al. (2017b, and references there-in), S5 0716+714: Chandra et al. (2011). In order to quantify the probability of variation in a source, duty cycle of variation (DCV) is often used. The DCV is defined as the fraction of total number of nights the source is monitored for, which are found variable (Romero et al. 1999). An expression to estimate DCV is given by,

$$DCV = 100 \frac{\sum_{i=1}^n (N_i / \Delta t_i)}{\sum_{i=1}^n (1 / \Delta t_i)} \% \quad (5)$$

where, $\Delta t_i = \Delta t_{i,obs}(1+z)^{-1}$ is duration of monitoring in rest frame of the source, and N_i is 0 or 1 depending on whether the source is non-variable or variable, respectively.

Several authors (Wagner & Witzel 1995; Chandra et al.

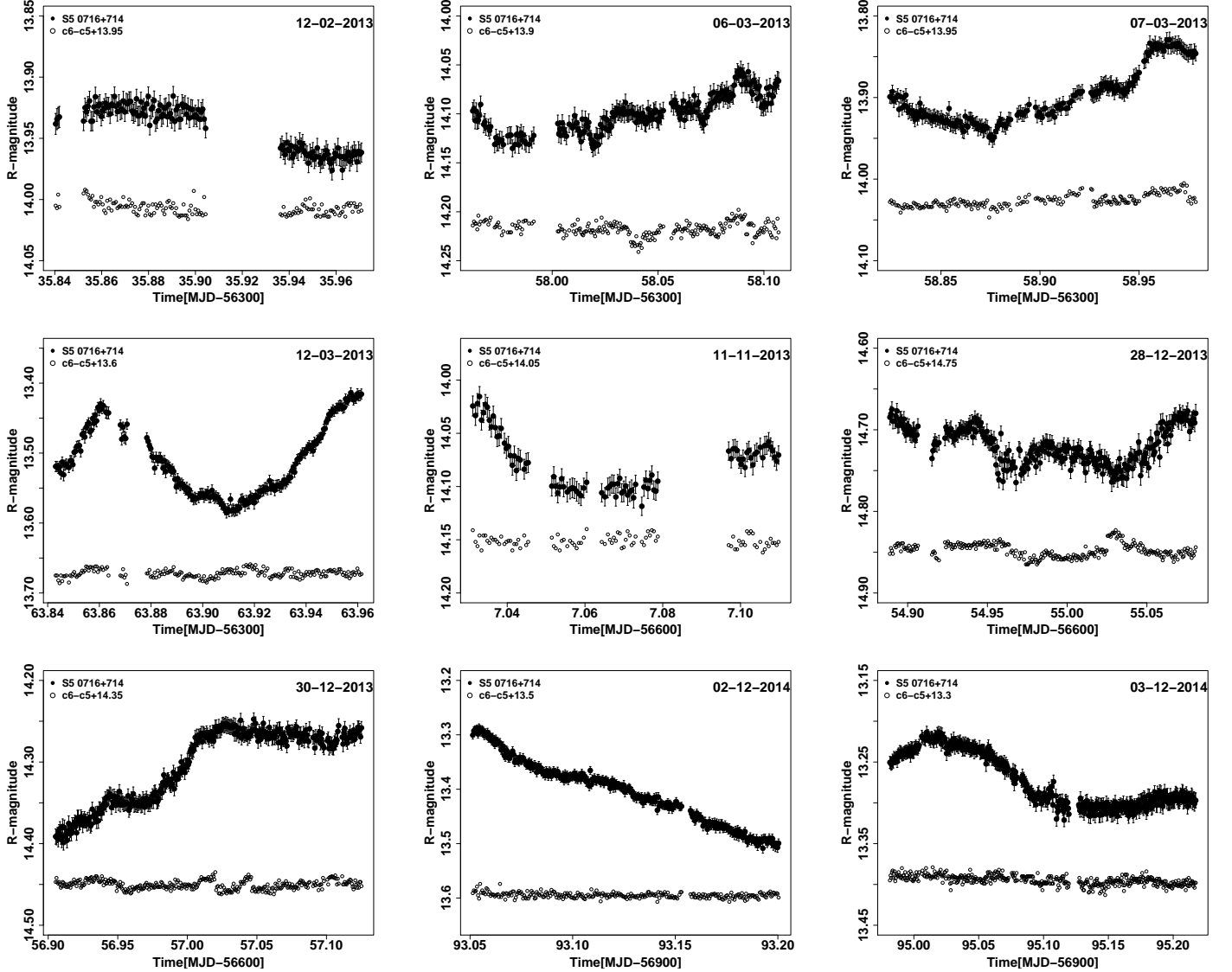


FIG. 1.— Intra-night light curves for the source S5 0716+714 on various nights during January, 2013 to June, 2015.

2011; Dai et al. 2015, and references there-in) have reported INV DCV for S5 0716+714 ranging from 40% to 100% during their observations, which indicates that the source is almost always active. In our case, 9-nights out of a total of 29 nights monitored for more than two hours, are detected as confirmed variable ones. Thus based on our observations during 2013-2015, we get a value of 31% as duty cycle, which is on the lower side. Reasons could be that we monitored the source, by chance, when it did not show much activity or our duration of monitoring may not be sufficient. Hong et al. (2018) monitored the source for less than one hour and reported a DCV of 19.57% and, in another study done over 13 nights during 2012 January-February, a value of 44% (Hong et al. 2017) was estimated, when the source was monitored for about 5-hours. In order to check for any connection between the INV shown by the source and the duration over which it was monitored, we calculated the duty cycle with more than one hour and two hour monitoring period.

Out of the total 46 nights of observation during 2013-

2015, we find 35 nights and 29 nights monitored for a minimum of one hour and two hours, respectively. Based on these, we obtained INV duty cycle values for the S5 0716+714 as 26% and 31%, respectively, in two cases. It, therefore, indicates that longer the duration of monitoring, higher will be the probability of finding a source variable, i.e., a higher DCV.

Rise & fall rates of variation in INV lightcurves: To investigate the extent of the intra-night variability of the source, we determined rate of change in magnitude (rise/fall) on each INV night for S5 0716+714 by fitting a line segment to light curves. These rates of variation are given in Table 1.

During our observations, 2013 February 12 and 2013 December 28 represent the nights with minimum and maximum rates of change in the magnitudes of the source with $0.015 \text{ mag hr}^{-1}$ and $0.381 \text{ mag hr}^{-1}$ (cf, Table 1), respectively. The rate of brightness change on 2013 December 28 happens to be one of the fastest for this source. Earlier, Chandra et al. (2011); Man et al. (2016) have

TABLE 1
 DETAILS OF THE RATES OF RISE/FALL IN THE MAGNITUDE FOR INV NIGHTS. Δm_+ , Δm_- REPRESENT THE SOURCE BRIGHTENING OR DIMMING, RESPECTIVELY.

Date	Trend	Rise/Fall mag (Δm_+ / Δm_-)	Duration (in minutes)	Rate= $\Delta m/\Delta t$ (mag/hr)
12-02-2013	Fall	0.05 (Δm_-)	198	0.015
06-03-2013	Flickering over a monotonic rise	0.08 (Δm_+)	>150	0.02
07-03-2013	Fall	0.05 (Δm_-)	72	0.03
	Rise	0.12 (Δm_+)	144	
12-03-2013	Sine like pattern	0.10 (Δm_+)	30	0.05
		0.20 (Δm_-)	72	
		0.20 (Δm_+)	72	
11-11-2013	Fall	0.08 (Δm_-)	> 72	0.04
28-12-2013	Fall with flickering	0.08 (Δm_-)	72	0.38
		0.02 (Δm_-)	> 20	
30-12-2013	Monotonic rise	0.14 (Δm_+)	144	0.07
02-12-2014	Monotonic fall	0.02 (Δm_-)	216	0.05
03-12-2014	Sine like	0.08 (Δm_-)	288	0.02

reported 0.38 mag/hr & 0.35 mag/hr rates, respectively. Rate of change in the brightness magnitude as high as 0.43/hr has been reported for the PKS 2155-304 (Sandrinelli et al. 2014). The source showed smooth decline in its brightness by 0.05 mag on February 12 with 7.60 % amplitude of variability. On 2013 March 6, S5 0716+71 became brighter by 0.08 mag in 3 hours with rapid fluctuations (few tens of minutes duration) superposed over the day-long trend showing 7.58% amplitude of variation in the light curve. On 2013 March 7, brightness decreases from 13.90 mag to almost 13.95 mag within an hour, after which source brightened by more than 0.1 mag in next 3 hours with a rate of change of 0.03 mag hr⁻¹ as mentioned in the Table 1. On 2013 March 12, light-curve shows a sine like feature, with rising (0.1 mag in 30 min) - declining (0.2 mag in 72 mins) - rising (>0.2 in about 72 min approx.) trends in brightness over the duration of more than three hours.

The light curve on 2013 December 28 showed sharp rise/fall magnitudes over two peaks and again showed a rising trend with overall change in magnitude by 0.38 mag hr⁻¹ (see Table 1). However, the features in the light curves are asymmetric in nature, which rules out variation being caused by extrinsic/geometric mechanisms. The variability in blazars is stochastic in nature at almost all timescales. The flares, therefore, appear to be produced independently and any similarity or difference might reflect different scales of particle acceleration and energy dissipation (Nalewajko et al. 2015). The variations in blazars are caused largely in the jet but it is difficult to ascertain whether these are intrinsic or geometric in nature. Intrinsic variations are dissipative and irreversible in time. Hence they should cause asymmetric flares. The geometric variations, on the other hand, are symmetric in time (Bachev et al. 2012) and achromatic in nature. The intrinsic variability could be due to fast injection of relativistic electrons and radiative cooling and/or escape of the particles or radiation from the emission zone. The symmetric flares, however, might result if cooling time scale is much shorter than the light crossing time (Chatterjee et al. 2012).

The INV LCs are, in general, asymmetric and complex indicating the random/turbulent nature of the flow inside the jet. Based on the visual inspection of these curves,

we identify three observed trends:

a) Rapid intra-night changes in the source flux, indicating to the violent, evolving nature of the shock formed in the jet. It might be either due to the presence of oblique shocks or instabilities in the jet. b) The steady rise or fall in the light-curve during a night indicates to the light crossing timescale to be shorter than the cooling time scale of the shocked region. It is when data series is shorter than characteristic time scale of variability. The cooling times shorter than light crossing time would have resulted in symmetric light-curves (Chiaberge & Ghisellini 1999; Chatterjee et al. 2012). c) The small-amplitude rapid fluctuations (asymmetric in shape) superimposed over slowly varying light curve suggest small scale perturbations in the shock front or oscillations in the hot-spots downstream the jet and may not be associated with size of the emission regions.

3.1.2. Variability timescale, size of emission region and black hole mass

It is important to know the characteristic timescale of intra-night variability which can constrain the emission size and structures of the blazar emission zones. If we consider the shape of the jet as conical close to its origin, the opening angle and the extent of vertical expansion of the jet can provide us a rough estimate of the location of emission region with respect to the supermassive black hole (Ahnen et al. 2017; Kaur et al. 2017a).

The rapid variations with duration of a few hours originate, perhaps, in the close vicinity of the central engine where jets are launched and might be caused by a combination of accretion disk instability, shock propagating within the jet, and/or particle acceleration and consequent radiative cooling near the base of jet (Ulrich et al. 1997). This assumption is also used to estimate the mass of the black hole, which is difficult to determine otherwise as BL Lacs do not show emission lines. Since the INV light curves are complex, we use statistical tools, described here, to discuss features in the intra-night light curves and estimate INV timescales and any possible quasi-periodicity.

Structure function: The structure function (SF) described by Simonetti et al. (1985); Gliozzi et al. (2001)

TABLE 2

DETAILS OF THE INV NIGHTS FOR THE SOURCE S5 0716+714 DURING 2013-2015. COLUMN 1 TO 11 PRESENT; DATE, MJD, OBSERVATION START TIME, DURATION, NO. OF IMAGES, AVERAGE MAGNITUDE WITH ERROR, TEST PARAMETER C, AMPLITUDE OF VARIATION, VARIABILITY TIME SCALE, SF PARAMETERS; k & β .

Date of observation	MJD	T_{start} (hh:mm:ss)	Duration (hrs)	N^a	$\bar{m} \pm \sigma$	C	A_{var} (%)	t_{var}	k	β
12-02-2013	56335.84038	20:10:09	3.28	195	13.94 ± 0.02	2.63	7.60	>2.36 hr	0.31	4.82
06-03-2013	56357.96250	23:06:00	3.46	237	14.10 ± 0.02	2.72	7.58	>1.68 hr	0.99	1.67
07-03-2013	56358.82424	19:46:54	3.71	203	13.90 ± 0.03	4.46	11.38	2.04 hr	1.71	1.81
12-03-2013	56363.84308	20:14:02	2.83	229	13.50 ± 0.05	8.90	15.61	1.11 hr	0.08	1.21
11-11-2013	56607.03115	00:44:51	1.88	139	14.08 ± 0.02	4.62	9.75	0.96 hr	3.61	1.33
28-12-2013	56654.88889	21:20:00	2.48	284	14.72 ± 0.02	2.65	11.89	0.76 hr	1.14	0.97
30-12-2013	56656.90536	21:43:43	2.26	350	14.30 ± 0.05	7.55	15.38	3.1 hr	0.88	1.31
02-12-2014	56993.05133	01:13:05	4.58	284	13.41 ± 0.06	12.37	20.50	3.54 hr	2.29	2.34
03-12-2014	56994.98155	01:13:55	5.97	454	13.27 ± 0.03	5.23	10.07	3.89 hr	2.32	2.41

^aNumber of data points

provides information about characteristic timescale of variability for flat- and steep spectrum radio sources by analyzing their light curves. In order to estimate the characteristic variability timescale, we used first order structure function for a magnitude data series, defined as,

$$SF(\tau_i) = \frac{\sum [M(t + \tau_i) - M(t)]^2}{N} \quad (6)$$

where, $M(t)$ is the magnitude at time t and τ_i is the time lag. The chi-square method is used to fit the structure function where from minimum variability timescale and corresponding errors are estimated (Zhang et al. 2012). The SF reveals extent of changes in the magnitude as a function of time between two observations. In this curve of growth of variability with time lag, a plateau (change of slope or saturation of SF) might indicate presence of a characteristic time.

$$SF(\tau) = \left\{ \begin{array}{l} k\tau^\beta, \quad \tau \leq \tau_o, \\ C, \quad \tau > \tau_o. \end{array} \right\} \quad (7)$$

where, τ_o is characteristic timescale with 1σ uncertainty and $\beta = \frac{d \log(F)}{d \log(\tau)}$ is logarithmic slope in $\tau - SF$ plane characterizing the nature of the variability and physical processes. If the value of β is close to 0, it indicates flickering noise, while $\beta \geq 1$ indicates turbulent process in jet (or shot-noise) responsible for the changes.

Figure 2 shows the structure functions for the INV nights. It is seen that first order SF for several nights does not show any plateau, that means that the characteristic timescale of variability is longer than the length of the observational data (Dai et al. 2015). The local maximum following the smooth rise in the SF- τ plane reveals time-scale of variability introduced by the presence of minimum and maximum or vice-versa in the curve. If the SF consists of more than one plateau with slopes (β) following a power-law trend, presence of multiple timescales is inferred. If periodicity is present, it will be seen as local minima in SF after the occurrence of a local maximum. The difference between two minima gives the time period.

On several nights (2014-12-02, 2013-03-07, 2013-11-11, & 2013-02-13), SF shows continuous increase with no or a feeble plateau, indicating that characteristic time scale of variability is longer than the monitoring period, giving only a lower limit of the variability time scale. While LC for the night 2013 March 12 shows several features, SF shows only one plateau and then a dip at about 2.2 hr. On December 13, 2013, SF shows a discernible peak with a time scale of 3.11 hr, followed by a rise. SF for INV night of 2014 December 14 shows a plateau at 2.89 hr. As can be seen, INV night 2013 December 28 shows a plateau in its SF giving the shortest characteristic timescale of variability of about 45.6 minutes during our observing campaign.

The quantitative values of various parameters related to INV nights, including SF parameters, are given in Table 2. In this table, the column 1 and 2 represent the date of observation (in dd-mm-yyyy and MJD format, respectively), column 3 represents the start time of the observations, the duration of monitoring and the number of data points (images) are given in column 4 and 5, column 6 presents the average magnitude and the associated errors in the source brightness, column 7 and 8 contain the values of the statistical parameters, i.e., C and A_{var} , respectively. The variability timescales for INV nights are shown in column 9 along with the structure function parameters, normalization constant(k) and logarithmic slope(β) in columns 10 & 11, respectively.

The INV lightcurves feature several complete events with specific time scales. Applying light travel time arguments, these time scales can be used to put limits on the size of the emission regions responsible for the variation in flux. The shortest characteristic timescale puts constraint on the size of emission region (Elliot & Shapiro 1974). Using the characteristic timescales obtained from light curve and SF analysis, the size of the emission region,

$$R \leq \frac{\delta c \Delta t_{var}}{(1+z)} \quad (8)$$

where, c is speed of light, Δt_{var} is minimum timescale

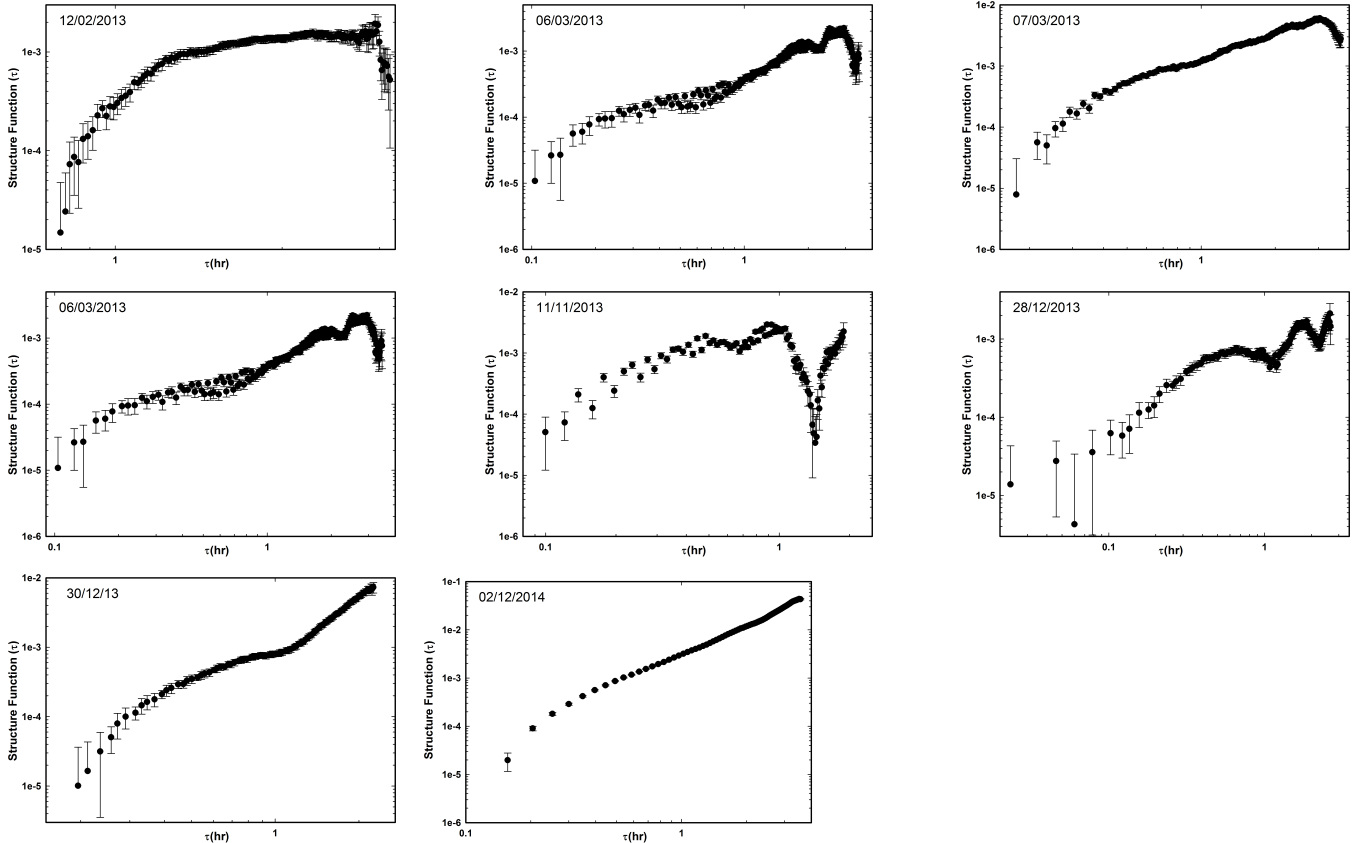


FIG. 2.— Structure functions for the INV nights are plotted for the source S5 0716+714 during 2013-2015. X-axis represents time lag in hours.

of variability, δ is the Doppler factor and z is the redshift of the source ($z=0.32$). When considering long-term behaviour, various authors have used different values of the Doppler factor, δ . [Bach et al. \(2005\)](#) use Doppler factors 13 to 25 when viewing angle changes from 5° to $0^\circ.5$. [Nesci et al. \(2005\)](#) adapted a value of 20, while [Fuhrmann et al. \(2008\)](#) apply a range 5 to 15 for the Doppler factor. We have used a value of 15 in this work, taking into account the brightness of the source during the observed period. Thus, using $\Delta t_{var} = 45.6$ minutes as the characteristic time scale of variability, the estimated size of the emission region is of the order of $\approx 10^{15}$ cm. Apart from this shortest time scale of variability, other time scales estimated on other nights indicate different sizes of emission regions in the jet. The longest time scale of variability detected in the present study is 3.89 hr which corresponds to a size of 4.8×10^{15} cm in the source frame. All these emitting regions are very compact and close to the black hole, within the BLR region.

Mass is one of the most important properties of a black hole. There are two categories of methods to determine the mass of a black hole in AGN; primary and secondary. While there are direct, primary methods applicable to nearby black hole systems where motion of the surrounding stars and gas under the influence of black hole, are traceable ([Vestergaard 2004](#)), it is very difficult to have an estimate of their masses at high redshifts. In the secondary methods, mass of the black hole is estimated by resorting to approximations, e.g., using a parameter with which black hole mass is correlated. There are several methods which fall into this category. However, for the

sources which do not show any emission line and whose host galaxy is also weak/non-detectable, which is the case for BL Lac type sources, it becomes extremely difficult to estimate the mass of black hole. For such systems, the variability time scale can provide a rough estimate of the black hole mass, assuming that the shortest time scale of variation is governed by the orbital period of the inner most stable orbit around a Kerr (maximally rotating) black hole. [Miller et al. \(1989\)](#) claim the origin of microvariability to arise from a location very close to the central engine based on the fast variability time scales, while [Marscher et al. \(1992\)](#) associate their location somewhere down the jet and perhaps near the sub-mm core, caused by turbulence.

Many authors have estimated masses of black holes residing in the BL Lac sources following the earlier ([Miller et al. 1989](#)) approach using shortest variability time scales ([Fan 2005](#); [Gupta et al. 2008](#); [Rani et al. 2010](#); [Chandra et al. 2011](#); [Kaur et al. 2017b](#); [Xie et al. 2002](#); [Liang & Liu 2003](#); [Dai et al. 2015](#)). Here we use this method to estimate the mass of a Kerr black hole at the center of S5 0716+71 using the expression ([Abramowicz & Nobili 1982](#); [Xie et al. 2002](#))

$$M = 1.62 \times 10^4 \frac{\delta \Delta t_{min}}{1+z} M_\odot, \quad (9)$$

where, c is the speed of light, z , the redshift and δ is the Doppler factor. Taking the shortest variability time scale, $\Delta t_{min} = 45.6$ min and Doppler factor as 15, we estimate the mass of the Kerr black hole to be $5.6 \times 10^8 M_\odot$,

which is in close agreement with other values including a value of $1.25 \times 10^8 M_\odot$ (Liang & Liu 2003) obtained by using optical luminosity. Bhatta et al. (2016) linked plateau in the *LC* to the characteristic timescale for developing outflow within the jet base, equivalent to the innermost stable orbit and obtained the value of black hole mass as 4×10^9 (maximally spinning BH) and $3 \times 10^8 M_\odot$ (lowest spin BH). Agarwal et al. (2016) obtained a value of $2.42 \times 10^9 M_\odot$ for the black hole mass in S5 0716+714. Hong et al. (2018) estimated mass of the black hole as $5 \times 10^6 M_\odot$ using 50 min QPV originated from the inner most orbit of the accretion disk. Using the black hole mass, M_{BH} , estimated here, the Eddington luminosity can be estimated from the following expression given by Wiita (1985),

$$L_{Edd} = 1.3 \times 10^{38} (M/M_\odot) \text{erg s}^{-1} \quad (10)$$

which, in case of the S5 0716+71 comes out to be about $7.28 \times 10^{46} \text{erg s}^{-1}$.

Quasi-periodic variability: Another very interesting albeit highly debatable issue is the possible presence of periodicity in the blazar light curves. Claims for their existence have been made in optical bands (Lainela et al. 1999; Fan & Lin 2000). A few INV *LC*s indicate the presence of possible quasi-periodic variations, also noticed in this source by Wu et al. (2005); Gupta et al. (2008); Rani et al. (2010); Poon et al. (2009); Man et al. (2016), with periods varying from 15 minutes to 1.8 hr. The presence of such features, if genuine, can be explained by the lighthouse effect (Camenzind & Krockenberger 1992), plasma moving in a helical magnetic field or micro-lensing effect etc. Recently Hong et al. (2018) obtained 50 min QPV from the observations during 2005 - 2012 when S5 0716+71 was in a relatively fainter state. They opined that the QPV is caused by the activity in the inner most orbit of the accretion disk. In the present case, the variations seen on timescales of a few hours with asymmetric profiles rule out the possibility of the micro-lensing as the mechanism. Here, flares could be caused by a sweeping beam whose direction changes with time due to helical motion. To estimate variability timescales and/or periodicity (if present) in our *LC*s, we use structure function and periodogram analysis.

The SF for the night of 2013-03-12 shows only one minima at about 2.2 hr while that for 2013-12-28 gives two minima at 1.25 hr and 2.3 hr, giving a possible period of about 1.2 hr.

However, since these periods are either closer to the length of the data series and/or flux enhancements are less than 3σ , existence of periodicity is doubtful. Also, these features may not significantly represent departure from a pure red-noise power spectrum. Though the quality of the light curve presented here, in particular its dense sampling, is good enough for a search of hour-long QPVs, the fact that we did not find such QPV at a significantly high level to claim the detection, is meaningful in itself. It implies that no persistent periodic signal exists in the source within the analyzed variability timescale domain.

3.1.3. Variability amplitude (A_{var}) and the brightness state of source

In order to find out whether extent of variability has any dependence on the brightness of the source, we calculated the amplitude of variability (A_{var}) in R-band for all the nights monitored for long enough time to show a minimum of 3% amplitude variation (see Equation 4). The values of A_{var} are plotted against nightly averaged brightness magnitudes in R-band (Figure 3) for the duration of 2013 January to 2015 June. We notice larger variability amplitudes when the source was brighter. In blazars, the A_{var} is indicative of the environment where turbulent plasma in the jet interacts with frequent shock formations where relativistic electrons are accelerated in the magnetic field which then cools down leading to synchrotron radiation. During this period (2013-2015), the source was in a relatively more active phase showing average R-band magnitude of $13.22 \pm 0.01 \text{mag}$ (historical average $R = 14.0$) and therefore one would expect larger amplitude of variation in the active jet. When the source is relatively faint, thermal emission from the host galaxy is expected to dilute the intrinsic variation in the jet emission, resulting in smaller A_{var} . Several authors have reported a similar behaviour to what we have noticed. Agarwal et al. (2016) and Yuan et al. (2017) notice a very mild trend of larger A_{var} when the source was brighter. Montagni et al. (2006) estimated rates of magnitude variation for 102 nights during 1996–2003 for S5 0716+71 and found faster ($\sim 0.08/h$) rates when source was brighter ($R < 13.4$), though the dependence was weak, compared to average rate of change ($\sim 0.027 \text{mag/h}$) irrespective of the state of the source brightness.

However, just the opposite behaviour has been detected by Kaur et al. (2017b) in another IBL, 3C66A, i.e., larger amplitude of variability when the source was relatively fainter. Similar trend was reported by Chandra (2013); Baliyan et al. (2016) in a long-term (2005- 2012) study on the blazar S5 0716+714, reporting larger amplitude of variation when source was relatively fainter. Perhaps more extensive study on several blazars is needed to address this issue.

The behaviour of amplitude of variation as a function of the source brightness also provides a clue to how the LTV and INV could be related. When the source is bright, it indicates that the relativistic shock is propagating through the larger scale jet leading to enhanced flux at the longer time scale (LTV) Romero et al. (1999). The interaction of the shock with local inhomogeneities (small scale particle or magnetic field irregularities) or turbulence interacting with the shock (Marscher et al. 1992) is perhaps giving rise to the intra-night variations (INV). Since we notice an increase in the amplitude of INV with an increase in the mean brightness of the source, later being seen due to LTV, there is perhaps a relation between LTV and INV. A statistical study on a number of sources with good quality long-term data showing INV, STV and LTV on a large number of nights would, perhaps reveal whether INV amplitudes really have any correlation with the long and short term variability amplitudes. Certainly, S5 0716+714 would qualify as one such candidate for the study.

3.2. Long-term variability

The long-term optical light curve constructed for the period 2013 January-2015 June for the S5 0716+714 is

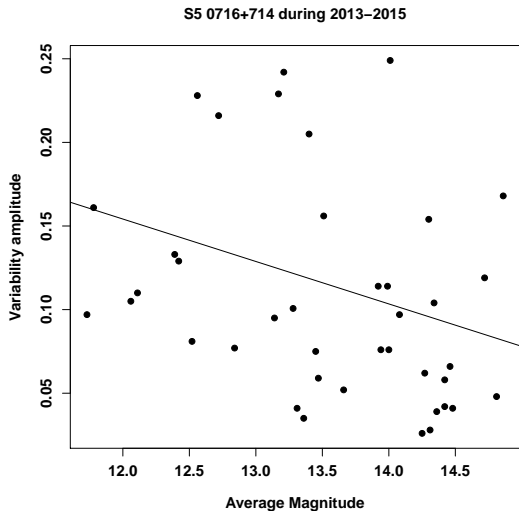


FIG. 3.— The amplitude of variability as a function of the average R-band brightness during 2013–2015.

shown in Figure 4, with time in MJD and B,V,R & I brightness in magnitude. A total of 46 nights with 6256, 159, 214, & 177 data points in R, B, V, & I-bands, respectively, are used in generating these *LC*s. The source was in its faintest state with 14.85(0.06) mag in R-band on MJD 56663.02 (2014 Jan 6) and in its brightest state with 11.68(0.05) mag, almost one year later on MJD 57040.90 (2015 January 18). S5 0716+71 has undergone several outbursts and flares during its two & half year journey with two major outbursts peaking in 2013 March and 2015 January, having a duration of about 350 & 510 days, respectively (see Figure 4). An outburst here is defined as a significant (more than one magnitude) enhancement in the flux over a considerable duration- tens of days to a few months or longer. In our case, limited by the observational data (ours and those from Steward Observatory), we have estimated the outburst duration, looking at the trend of long term variation, based on the above criterion. These outbursts are superposed by a number of fast flares. We estimate long-term variability (LTV) amplitudes of about 2.5 mag and 3.45 mag with time scales of 250 and 360 days, respectively, during these two outbursts. These LTV time scales are estimated with respect to the minimum and maximum brightness values of the source during the two outbursts. During the 2015 January outburst, S5 0716+714 reached its unprecedented brightness level (Chandra et al. 2015a,b). Using multi wavelength data from Fermi-LAT, Swift-XRT, Swift UVOT, MIRO (optical R-band), Steward optical R-band and polarization data, we (Chandra et al. 2015b) detected two sub-flares contributing to this major 2015 January outburst. In optical, the source brightened by 0.8 mag in 6 days (MJD 57035–57041) and, post flare, decayed over next four days at a rate of 0.13 mag per day. Very sharp drop in brightness within a day (MJD 57040–57041) and subsequent rise in brightness the very next day (MJD 57042) indicated to the presence of two sub-flares with almost same peak flux during the outburst. A rapid swing in the position angle of polarization indicated to the magnetic reconnection (Zhang et al. 2012) in the emission region, causing the outburst.

In the long term, the source became fainter within a

year from its average brightness, $R = 13.5$ mag in 2013 to $R \sim 15$ mag in 2014 January. It was then in the brightening phase during 2014 to 2015 with intermittent flaring activity. S5 0716+71 attained brightest flux value in 2015 January and started its journey towards fainter side later as reflected in all the B, V, R, and I-band (from $R = 11.68$ mag to 13.20 mag, a 1.52 mag decay in five months, c.f., Figure 4) *LC*s. In addition to major outbursts, there are at least 9-flares with their duration ranging from 20 days to 30 days leading to changes in brightness of the source from a few tenths of magnitude to as much as more than 1.5 magnitude in R-band. The frequent large gaps in the data restrict us from appropriately characterizing these flares which indicate that the source remains almost always active with substantial brightness changes. During our observation period, S5 0716+714 was brightest on 2015 January 18 (MJD= 57040.90) with a value $R= 11.68 \pm 0.05$ and faintest on 2014 January 06 (MJD=56663.02) with a value $R=14.85 \pm 0.06$.

There are several approaches to explain the variation at various time scales- long as well as short. The intrinsic variations could be caused by the instability & hot spots in the disk or its outflow (Kawaguchi et al. 1998; Chakrabarti & Wiita 1993), and activities in the relativistic jet (Marscher & Gear 1985; Marscher 2008). Variations could also be caused by the processes extrinsic to the source, e.g., interstellar scintillation- which are highly frequency dependent and normally affect long wavelength radio observations, gravitational microlensing - might cause long-term variations in some source but will result in achromatic, symmetric lightcurves. The later is less likely to cause INV (Wagner & Witzel 1995). Since S5 0716+714 was in a relatively bright phase and emission is strongly jet dominated, most probable source of variation should be processes in the jet. The shock-in-jet model (Marscher & Gear 1985; Marscher 2008) is normally able to explain a variety of variability events with some modifications (Zhang et al. 2015; Camenzind & Krockerberger 1992), where a shock propagates down the jet interacting with a number of particle over-densities or stationary shocks/cores distributed randomly in the parsec scale jet. Such standing shocks are formed due to pressure imbalance between jet plasma and interstellar medium (ISM). In trying to maintain a balance, an oblique shock is created perpendicular to the jet axis. The relativistic shocks interacting or passing through such regions energize the particles in the presence of magnetic field, which then radiate synchrotron emission while cooling. Either the jet moves in a helical motion or the blob moves in a helical magnetic field, causing a change in the viewing angle, thus changing the Doppler factor which significantly enhances/reduces the intrinsic flux variation, depending upon the decrease/increase in the angle. The model can explain rapid variations by resorting to a jet-in-jet scenario (Zhang et al. 2015; Camenzind & Krockerberger 1992). The small flares before the outburst indicate acceleration/cooling of the relativistic particles due to plasma blobs interacting with shock front and an ongoing activity in the jet due to the superposition of all the events leading to long-term variability in the source. In our study, after the second outburst, the source enters into a faint state again.

Several studies have been carried out to address the long-term behaviour of the source. (Raiteri et al. 2003;

Nesci et al. 2005) used the historical data, including from the literature, during 1953–2003 and noticed alternate trends of decreasing and increasing mean brightness on a tentative period of about 10 years, claiming precession of the jet to be responsible for them. It should be noted that even during these slow trends of increasing/decreasing mean brightness levels, source was very active with a large number of flares superposed on the longer trends. Again, a decreasing trend was noticed by Chandra (2013) beginning 2003 which continued upto 2012, they also predicted an increase in average brightness after 2014. Agarwal et al. (2016) observed the source for 23 nights during 2014 November– 2015 March and found the source in bright state, showing INV for 7 out of 8 nights and STV with 1.9 mag change during about 28 days (MJD 57013.86 – 57041.34). In their long-term work for the period 2004 – 2012, Dai et al. (2015) reported STV at 10 days time scale, 11 INV nights out of 72 nights observed with an average magnitude of $R=13.25$ and an overall change by 2.14 magnitude.

A complete observation log along with daily averaged R band photometric magnitudes for S5 0716+714 and nature of the night, are provided in Table 3.

3.2.1. Spectral behavior of S5 0716+71

The variation of color with the brightness of the source provides useful clues to constrain the blazar emission models (Hao et al. 2010). To investigate the spectral behavior of S5 0716+714 over long timescale i.e., from 2013 to 2015, the color-magnitude diagrams, (B-R) v/s R, (B-V) v/s V and (V-R) v/s R, are plotted using nightly averaged magnitudes in B, V and R bands, respectively. The minimum and maximum values of the colour indices for better sampled case of B-R v/s $(B+R)/2$ are, 0.40 and 1.3, respectively, while the color average is $\langle B - R \rangle = 0.6$ mag, with standard deviation $\sigma=0.14$ mag. The Figure 5 shows the spectral behavior of the source with the brightness during 2013–2015. The first panel (from top) shows the (B-R) spectral color versus its average magnitude. Similarly, the middle and the bottom panels display the (B-V) and (V-R) spectral behavior with their average brightness magnitudes, respectively. To quantitatively determine the correlation between the color index with brightness in Figure 5 (Color v/s magnitude), we performed regression analysis by fitting a straight line, $y = mx + c$ (y = color index, x = average magnitude) using linear model in R software package and extracted various parameters, such as, intercept(c), slope(m), correlation coefficient(r), p-value etc. The values for these parameters are given in Table 4.

It is clear from the Figure 5 and values of various parameters obtained from regression analysis (see Table 4) that the source showed weak positive correlation for B-V and V-R color indices plotted against brightness magnitudes, with Pearson correlation coefficient (r) of 0.25 and 0.35 along with p-value of 0.29 and 0.13 respectively. However, comparatively stronger positive correlation for B-R color index versus average magnitude of source with Pearson coefficient r as 0.5 and null hypothesis probability, $p = 0.02$ are noticed. Thus present study suggests a bluer-when-brighter (BWB) color for S5 0716+71 (cf., Figure 5) as also reported by many workers (Poon et al. 2009; Chandra et al. 2011; Wu et al. 2009; Man et al.

2016). Li et al. (2017) statistically studied the data for S5 0716+71 during 1995-2015 and addressed the issue of long-term, short-term and INV behaviour of the symmetry in flares and color and found flares as asymmetric in general and BWB color on all the time scales considered. The spectral changes in S5 0716+714, and blazars in general, are complicated and difficult to explain. The source was reported with strong BWB trend over long-timescales (Poon et al. 2009) and during its flaring phase (Ghisellini et al. 1997; Wu et al. 2005, 2009; Gu et al. 2006). Wu et al. (2005) and Agarwal et al. (2016) discussed color trends in their studies but did not find any change on the intra-night or long-term timescales. Raiteri et al. (2003), on the other hand noticed all possible scenarios, i.e., BWB, RWB and no trend at all, in their studies. Stalin et al. (2009) found source showing no color dependence with brightness on both - the long and short time scales, albeit a BWB color on intra- and inter-night timescales was noticed. The fresh injection of high energy particles in the emission region inside the jet might lead to BWB behaviour (Ghisellini et al. 1997; Raiteri et al. 2003; Gu et al. 2006). The BWB behaviour can be explained by the shock-in-jet model (Marscher & Gear 1985; Marscher 2008) where the propagation of a disturbance downstream the jet gives rise to the shock formation and the lag between the emissions at different wavelengths provides information on their relative spatial separations. In the case of BL Lacs, the higher frequency electrons close to the shock front undergo faster radiation losses than the low-frequency ones. The BWB behavior basically means that the flux enhancements are produced either during the episodes of intense particle acceleration or, alternatively, by the fluctuating magnetic field superimposed on the local, steady electron energy distribution. The redder when fainter trend indicates that when the jet is not dominant, the contribution from the disk emission or the host galaxy becomes relevant. These cases show the complex color behaviour of the source with brightness. However, in case of the S5 0716+714 where host galaxy is several magnitudes fainter, $R > 20$ mag (Montagnani et al. 2006), thermal contribution from the host is negligible.

Spectral variation with time: The long-term optical light curves of blazars manifest significant details on the nature of the source as these contain various phases in their brightness, color changes during flares, outbursts and fainter states. Several authors have looked at spectral variations with time on intra-night and inter-night timescales for blazars (Raiteri et al. 2003; Wu et al. 2005; Stalin et al. 2009; Gaur et al. 2012; Rani et al. 2010; Agarwal et al. 2016) and reported a mixed behaviour- some sources showing color dependence while others showed no change in color over considered timescales. Agarwal et al. (2016), during their 130 day study, found a change of about 0.3 mag in spectral color with no significant dependence on the time or brightness phase. Yuan et al. (2017) reported a complex pattern for spectral index with time without any specific trend during the period 2000-2014. The color variations are caused by differential cooling of energetic electrons behind the shock front. The relativistic shock moving down the jet accelerates electrons to high energies at the sites of high magnetic field or electron density giving rise to emission at

TABLE 3

OBSERVATION LOG AND PHOTOMETRIC RESULTS FOR S5 0716+714 IN R-BAND DURING 2013 JANUARY-2015 JUNE. COLUMNS ARE: DATE OF OBSERVATION, TIME (UT) & MJD, NO. OF DATA POINTS, AVERAGE MAGNITUDE WITH STANDARD DEVIATION & PHOTOMETRIC ERRORS, VARIABLE (Y/N)

Date (dd-mm-yyyy)	T_{start} (hh:mm:ss)	MJD	N^a	\bar{m} (Avg mag)	$m(\sigma)$ mag	E_{phot} mag	Variable (Y/N)
14-01-2013	21:30:14	56306.89600	785	13.478	0.01	0.01	N
12-02-2013	20:10:09	56335.84038	195	13.943	0.02	0.01	Y
06-03-2013	23:06:00	56357.96250	237	14.007	0.10	0.03	Y
07-03-2013	00:03:50	56358.00266	203	13.996	0.10	0.01	Y
10-03-2013	19:37:50	56361.81794	231	13.356	0.01	0.003	N
12-03-2013	20:14:02	56363.84308	229	13.505	0.05	0.004	Y
13-03-2013	23:38:51	56364.98531	160	13.660	0.01	0.005	N
11-04-2013	19:49:09	56393.82580	182	12.563	0.03	0.02	N
12-04-2013	19:46:43	56394.82411	5	12.780	0.02	0.02	N
11-11-2013	00:44:51	56607.03115	139	14.078	0.02	0.003	Y
26-11-2013	03:20:25	56622.13918	13	14.310	0.01	0.003	N
27-11-2013	01:48:39	56623.07545	25	14.259	0.01	0.01	N
28-11-2013	01:13:25	56624.05098	169	14.275	0.01	0.01	N
29-11-2013	01:07:09	56625.04663	247	14.337	0.01	0.01	N
30-11-2013	02:29:12	56626.10361	107	14.357	0.01	0.008	N
01-12-2013	03:08:06	56627.13063	112	14.485	0.01	0.02	N
02-12-2013	02:32:13	56628.10571	200	14.417	0.01	0.04	N
03-12-2013	02:12:03	56629.09170	242	14.463	0.01	0.03	N
05-12-2013	00:19:24	56631.01347	230	14.011	0.03	0.02	N
28-12-2013	21:20:00	56654.88889	284	14.718	0.02	0.007	Y
30-12-2013	21:43:43	56656.90536	350	14.304	0.04	0.005	Y
01-01-2014	00:18:37	56658.01293	183	14.423	0.01	0.004	N
05-01-2014	02:10:57	56662.09094	50	14.816	0.01	0.005	N
06-01-2014	00:43:03	56663.02990	349	14.855	0.06	0.006	N
26-04-2014	20:26:39	56773.85184	10	13.924	0.05	0.006	N
27-04-2014	20:08:22	56774.83914	05	13.969	0.01	0.008	N
22-11-2014	20:08:34	56983.83929	49	13.143	0.02	0.002	N
23-11-2014	18:47:49	56984.78321	207	13.212	0.06	0.005	N
02-12-2014	01:13:55	56993.05133	284	13.404	0.06	0.01	Y
03-12-2014	01:16:34	56994.05317	454	13.276	0.04	0.006	Y
22-12-2014	01:41:07	57013.07022	579	13.456	0.08	0.01	N
18-01-2015	18:15:04	57040.90131	105	11.681	0.05	0.05	N
19-01-2015	16:32:33	57041.68927	442	12.114	0.02	0.006	N
20-01-2015	18:49:11	57042.78417	06	12.087	0.04	0.002	N
22-01-2015	14:42:59	57044.61319	100	12.063	0.02	0.004	N
23-01-2015	16:37:47	57045.69292	934	11.776	0.03	0.004	N
24-01-2015	22:06:24	57046.92112	240	11.727	0.02	0.01	N
28-01-2015	17:19:42	57050.72202	557	12.398	0.02	0.002	N
29-01-2015	19:03:20	57051.79399	401	12.518	0.01	0.01	N
30-01-2015	15:40:12	57052.65292	513	12.416	0.02	0.01	N
31-01-2015	16:35:46	57053.69152	727	12.726	0.05	0.01	N
01-02-2015	20:38:28	57054.86005	44	12.837	0.02	0.01	N
25-05-2015	21:49:50	57167.90961	02	12.979	0.07	0.005	N
27-05-2015	20:35:16	57169.85782	05	12.626	0.01	0.02	N
30-05-2015	20:38:38	57172.86016	10	13.449	0.04	0.01	N
31-05-2015	20:22:47	57173.84916	15	13.315	0.01	0.003	N
01-06-2015	20:13:27	57174.84267	18	13.171	0.05	0.003	N

^aNumber of data frames

TABLE 4

THE VALUES OF THE REGRESSION PARAMETERS FOR COLOR INDICES AS A FUNCTION OF BRIGHTNESS FOR S5 0716+714 DURING 2013-15.

Color Index	m	c	r^2	r	p
B-R	0.08 ± 0.03	-0.22 ± 0.45	0.26	0.51	0.02
B-V	0.02 ± 0.02	0.16 ± 0.34	0.06	0.25	0.29
V-R	0.05 ± 0.03	-0.37 ± 0.48	0.12	0.35	0.13

m = Slope of regression line, r^2 = square of Pearson correlation coefficient, p = Probability for null hypothesis.

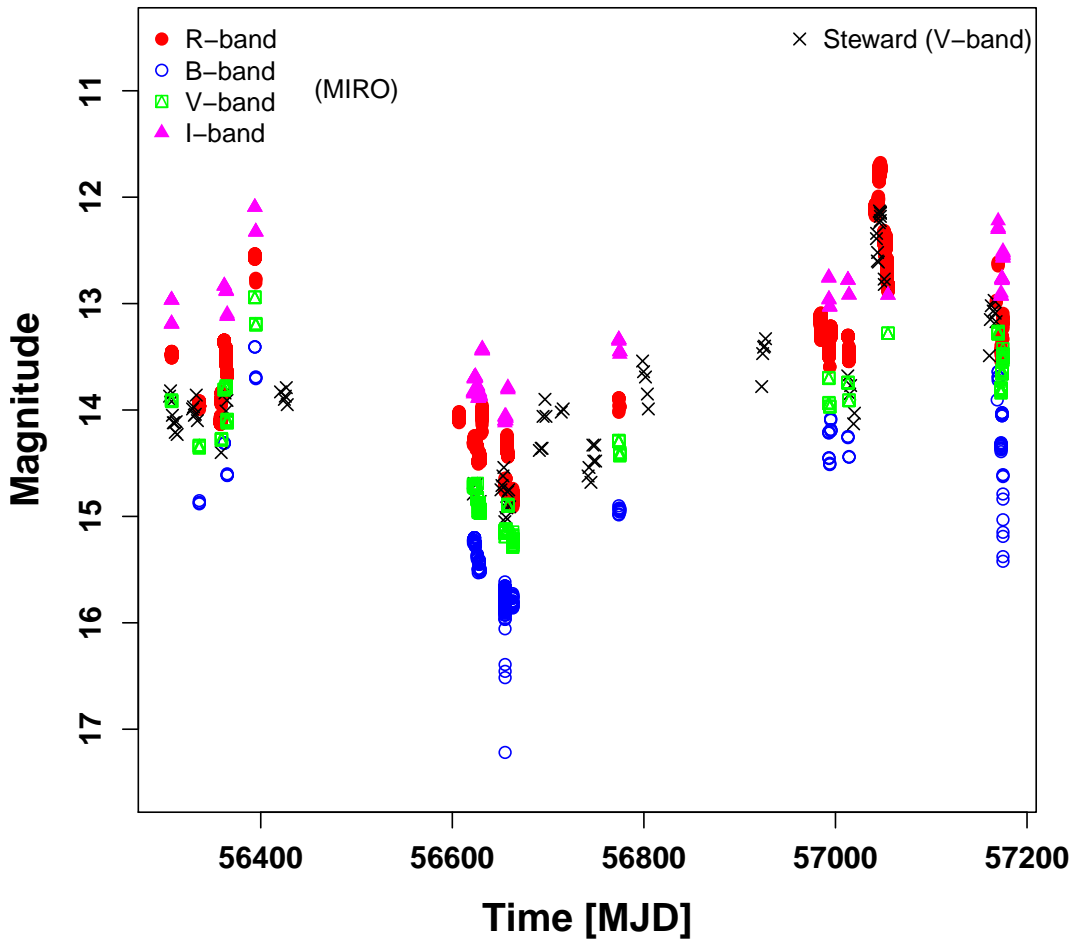


FIG. 4.— Long-term B, V, R & I band light curves of S5 0716+714 for the duration 2013 January - 2015 June. Data used are from MIRO and Steward observatory. The source has undergone in the brightest and the faintest phases, during 2013— 2015, exhibiting R-band magnitude of 11.68(0.05) and 14.85(0.06) respectively.

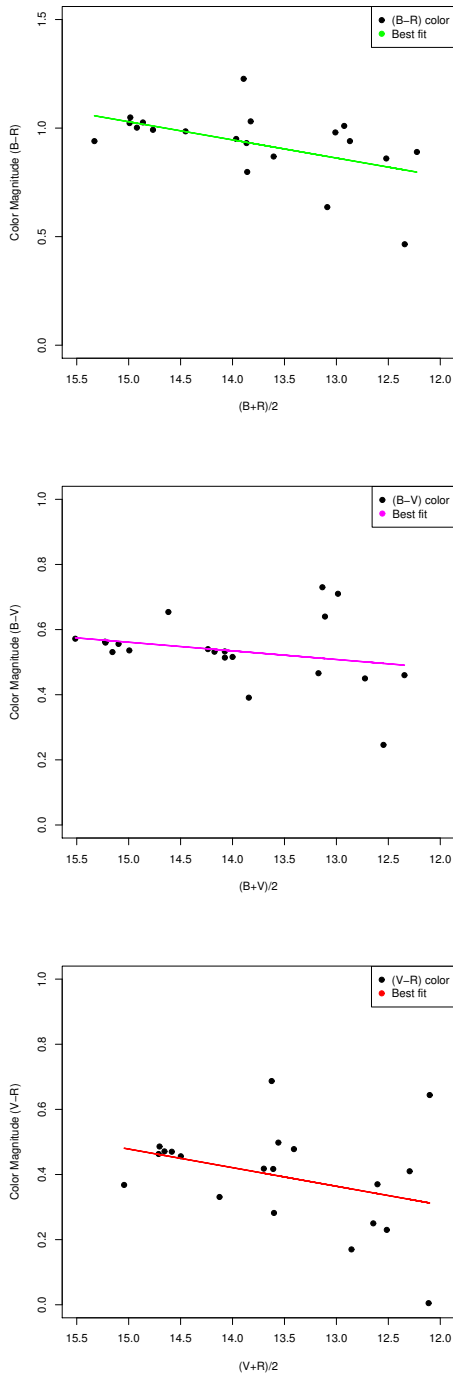


FIG. 5.— Color-magnitude plot for the source S5 0716+714 during 2013-2015, showing bluer when brighter trend. The fit is obtained by performing the linear regression analysis and values for the parameters are given Table 4.

diverse frequencies. In BL Lacs higher energy electrons cool faster with larger change in flux with time during a flare. Since the regions of the plasma over-densities or quasi-stationary shocks are randomly distributed in the jet, the interaction of the relativistically moving knot with existing features in the large scale jet gives rise to multiple outbursts which evolve individually and perhaps differently. The processes involved give rise to changes

in the spectral behaviour with time.

In order to understand the spectral behaviour of S5 0716+714 with time (2013 January to 2015 June), we plot color index (B-R), (B-V) and (V-R) against the time in MJD for this period in Figure 6. To get the correlation between the color index and time (MJD), we also performed regression analysis by fitting a straight line, $y = mx + c$ ($y =$ color index, $x =$ Time in MJD) using linear regression software package and extracted various parameters, such as, intercept(c), slope(m), correlation coefficient(r) and p-value. A nicely sampled lightcurve in different optical bands should give a clear picture of the temporal evolution of S5 0716+714. However, our data suffer from substantial gaps and the observations in different bands are not truly simultaneous.

The Figure 6 shows a mixed behaviour. While we notice a significant bluer spectral behavior with time in (B-V) color v/s time plot, indicating the source getting brighter at higher frequencies during this period of two and half years, we see very mild bluer trend in (B-R) v/s Time. However, the color index ($V - R$), shows a mild redder color with time. We, therefore, conclude, based on our data during 2013 January and 2015 June, that the source S5 0716+714 does not show any strong chromatic behaviour, barring (B-V) showing a bluer behaviour during this period. This mixed spectral behaviour with time is in line with other studies. The source was relatively in bright phase during 2013, in low-phase during 2014 and entered into its brightest phase in January 2015.

4. CONCLUSIONS

The IBL blazar S5 716 was observed for 46 nights with high temporal resolution during a period of more than two years (2013–2015) in optical BVRI wavelength bands from Mt. Abu InfraRed Observatory (MIRO). It was monitored for more than two hours during 29 nights to address INV. The nightly averaged B, V, R & I band brightness magnitudes with 6256, 159, 214 & 177 data points, were used to discuss long-term variability and color behaviour of the source. The source exhibited intra-night as well as inter-night variability at significant levels. From the present study, following conclusions are drawn:

- Source showed variability over diverse timescales i.e., a few tens of minutes to months and a duty cycle of variation of more than 31%. The DCV appears to be dependent upon monitoring time. Two major outbursts with ~ 370 and 500 days duration superimposed with several flares are noticed.
- The structure function analysis leads to the shortest variability timescale of 45.6 minutes, based on which upper limit on the size of emission region of the order of 10^{15} cm is estimated. There are several time scales longer than this indicating to multi-sized emission regions in the jet. Based on the longest time scale, the size of emission region is estimated as 4.8×10^{15} cm.
- Assuming the rapid variations to be originated in the vicinity of central engine, black hole mass is estimated to be $5.6 \times 10^8 M_{\odot}$ using shortest variability time scale.
- The structure function analysis is used to infer a

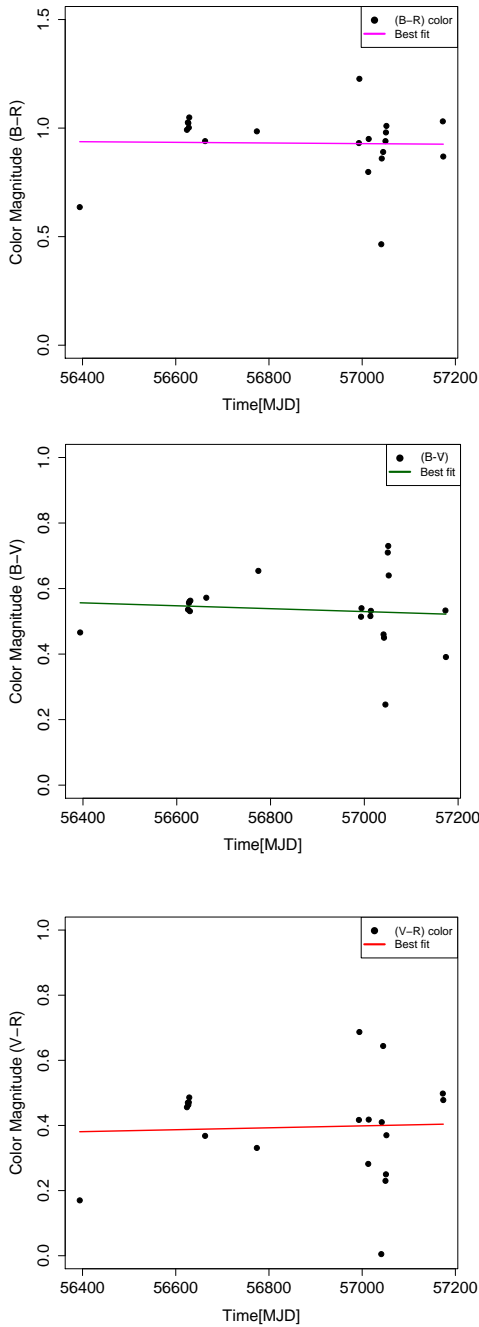


FIG. 6.— The color of the source S5 0716+714 plotted as a function of time (MJD) during 2013–2015. The continuous line is the best fit obtained using linear regression analysis of the data.

period of about 1.2 hr on the night of 2013 December 28. However, it could easily be red-noise signature as flux enhancements are within 3σ .

- The source exhibited a bluer when brighter (BWB) spectral behaviour in the long term LC which supports shock-in-jet model.
- The brightness of S5 0716+71 shows a mild increase with time during 2013 January–2015 June along with a mild bluer color.
- A larger amplitude of variation when the source was in relatively brighter state is detected, indicating to synchrotron dominated jet emission. It, perhaps, indicates that long-term and intra-night variabilities are linked.

It should be noted that these inferences are drawn from the data with large gaps. However, the data presented here should be very useful for other related statistical and modeling studies on this very interesting source.

5. ACKNOWLEDGEMENT

This work is supported by the Department of Space, Govt. of India. We are grateful to the anonymous learned referee for constructive remarks which improved the quality of this work. We express our thanks to Mr. Kumar Venkatramani and past observers as well as MIRO staff for their help in observations. We also acknowledge the use the data from the Steward Observatory spectropolarimetric monitoring project which is supported by Fermi Guest Investigator grants NNX08AW56G, NNX09AU10G, NNX12AO93G, and NNX15AU81G (Smith et al. 2009).

Facility:- MIRO:1.2m(PRL-CCD), MIRO:ATVS

REFERENCES

- Abdo, A. A., Ackermann, M., Ajello, M., et al. 2010, ApJ, 720, 912
- Abramowicz, M. A., & Nobili, L. 1982, Nature, 300, 506
- Agarwal, A., Gupta, A. C., Bachev, R., et al. 2016, MNRAS, 455, 680
- Ahnen, M. L., Ansoldi, S., Antonelli, L. A., et al. 2017, A&A, 603, A29
- Aliu, E., Archambault, S., Arlen, T., et al. 2012, ApJ, 759, 102
- Anderhub, H., Antonelli, L. A., Antoranz, P., et al. 2009, ApJ, 704, L129
- Bach, U., Krichbaum, T. P., Ros, E., et al. 2005, A&A, 433, 815
- Bachev, R., Semkov, E., Strigachev, A., et al. 2012, MNRAS, 424, 2625
- Bachev, R., Popov, V., Strigachev, A., et al. 2017, MNRAS, 471, 2216
- Baliyan, K. S., Kaur, N., Chandra, S., Sameer, S., & Ganesh, S. 2016, Journal of Astronomy and Space Sciences, 33, 177
- Bhatta, G., Stawarz, L., Ostrowski, M., et al. 2016, ApJ, 831, 92
- Biermann, P., Duerbeck, H., Eckart, A., et al. 1981, ApJ, 247, L53
- Blandford, R. D., & Königl, A. 1979, ApJ, 232, 34
- Böttcher, M. 2007, Ap&SS, 309, 95
- Camenzind, M., & Krockenberger, M. 1992, A&A, 255, 59

- Cellone, S. A., Romero, G. E., & Combi, J. A. 2000a, *AJ*, 119, 1534
—, 2000b, *AJ*, 119, 1534
Chakrabarti, S. K., & Wiita, P. J. 1993, *ApJ*, 411, 602
Chandra, S. 2013, PhD thesis, Department of Physics, MLSU, Udaipur, India
Chandra, S., Baliyan, K. S., Ganesh, S., & Joshi, U. C. 2011, *ApJ*, 731, 118
Chandra, S., Kushwah, P., Ganesh, S., Kaur, N., & Baliyan, K. 2015a, *The Astronomer's Telegram*, 6962, 1
Chandra, S., Zhang, H., Kushwaha, P., et al. 2015b, *ApJ*, 809, 130
Chatterjee, R., Baily, C. D., Bonning, E. W., et al. 2012, *ApJ*, 749, 191
Chiaberge, M., & Ghisellini, G. 1999, *MNRAS*, 306, 551
Ciprini, S., Takalo, L. O., Tosti, G., et al. 2007, *A&A*, 467, 465
Dai, B.-z., Zeng, W., Jiang, Z.-j., et al. 2015, *ApJS*, 218, 18
Danforth, C. W., Nalewajko, K., France, K., & Keeney, B. A. 2013, *ApJ*, 764, 57
Elliot, J. L., & Shapiro, S. L. 1974, *ApJ*, 192, L3
Fan, J.-H. 2005, *Chinese Journal of Astronomy and Astrophysics Supplement*, 5, 213
Fan, J.-H., Huang, Y., He, T.-M., et al. 2009, *PASJ*, 61, 639
Fan, J. H., & Lin, R. G. 2000, *ApJ*, 537, 101
Fossati, G., Maraschi, L., Celotti, A., Comastri, A., & Ghisellini, G. 1998, *MNRAS*, 299, 433
Fuhrmann, L., Krichbaum, T. P., Witzel, A., et al. 2008, *A&A*, 490, 1019
Gaur, H., Gupta, A. C., Strigachev, A., et al. 2012, *MNRAS*, 420, 3147
Ghisellini, G., & Tavecchio, F. 2009, *MNRAS*, 397, 985
Ghisellini, G., Villata, M., Raiteri, C. M., et al. 1997, *A&A*, 327, 61
Gliozzi, M., Brinkmann, W., O'Brien, P. T., et al. 2001, *A&A*, 365, L128
Gu, M. F., Lee, C.-U., Pak, S., Yim, H. S., & Fletcher, A. B. 2006, *A&A*, 450, 39
Gupta, A. C., Cha, S.-M., Lee, S., et al. 2008, *AJ*, 136, 2359
Hao, J.-M., Wang, B.-J., Jiang, Z.-J., & Dai, B.-Z. 2010, *Research in Astronomy and Astrophysics*, 10, 125
Heidt, J., & Wagner, S. J. 1996, *A&A*, 305, 42
Hong, S., Xiong, D., & Bai, J. 2017, *AJ*, 154, 42
—, 2018, *AJ*, 155, 31
Howell, S. B., & Jacoby, G. H. 1986, *PASP*, 98, 802
Howell, S. B., Warnock, III, A., & Mitchell, K. J. 1988, *AJ*, 95, 247
Jang, M., & Miller, H. R. 1997, *AJ*, 114, 565
Jorstad, S. G., Marscher, A. P., Larionov, V. M., et al. 2010, *ApJ*, 715, 362
Kaur, N., Chandra, S., Baliyan, K. S., Sameer, & Ganesh, S. 2017a, *ApJ*, 846, 158
Kaur, N., Sameer, Baliyan, K. S., & Ganesh, S. 2017b, *MNRAS*, 469, 2305
Kawaguchi, T., Mineshige, S., Umemura, M., & Turner, E. L. 1998, *ApJ*, 504, 671
Kuehr, H., Pauliny-Toth, I. I. K., Witzel, A., & Schmidt, J. 1981, *AJ*, 86, 854
Lainela, M., Takalo, L. O., Sillanpää, A., et al. 1999, *ApJ*, 521, 561
Larionov, V. M., Jorstad, S. G., Marscher, A. P., et al. 2013, *ApJ*, 768, 40
Laurent-Muehleisen, S. A., Kollgaard, R. I., Feigelson, E. D., Brinkmann, W., & Siebert, J. 1999, *ApJ*, 525, 127
Li, Y. T., Hu, S. M., Jiang, Y. G., et al. 2017, *PASP*, 129, 014101
Liang, E. W., & Liu, H. T. 2003, *MNRAS*, 340, 632
Man, Z., Zhang, X., Wu, J., & Yuan, Q. 2016, *MNRAS*, 456, 3168
Mannheim, K., & Biermann, P. L. 1989, *A&A*, 221, 211
Maraschi, L., Ghisellini, G., & Celotti, A. 1994, in *IAU Symposium, Vol. 159, Multi-Wavelength Continuum Emission of AGN*, ed. T. Courvoisier & A. Blecha, 221–232
Marscher, A. P. 2008, in *Astronomical Society of the Pacific Conference Series, Vol. 386, Extragalactic Jets: Theory and Observation from Radio to Gamma Ray*, ed. T. A. Rector & D. S. De Young, 437
Marscher, A. P., & Gear, W. K. 1985, *ApJ*, 298, 114
Marscher, A. P., Gear, W. K., & Travis, J. P. 1992, in *Variability of Blazars*, ed. E. Valtaoja & M. Valtonen, 85
Marscher, A. P., Jorstad, S. G., Larionov, V. M., et al. 2010, in *Bulletin of the American Astronomical Society, Vol. 42, AAS/High Energy Astrophysics Division #11*, 709
Miller, H. R., Carini, M. T., & Goodrich, B. D. 1989, *Nature*, 337, 627
Montagni, F., Maselli, A., Massaro, E., et al. 2006, *A&A*, 451, 435
Nair, S., Jin, C., & Garrett, M. A. 2005, *MNRAS*, 362, 1157
Nalewajko, K., Uzdensky, D. A., Cerutti, B., Werner, G. R., & Begelman, M. C. 2015, *ApJ*, 815, 101
Narayan, R., & Piran, T. 2012, *MNRAS*, 420, 604
Nesci, R., Massaro, E., Rossi, C., et al. 2005, *AJ*, 130, 1466
Nilsson, K., Pursimo, T., Sillanpää, A., Takalo, L. O., & Lindfors, E. 2008, *A&A*, 487, L29
Nottale, L. 1986, *A&A*, 157, 383
Poon, H., Fan, J. H., & Fu, J. N. 2009, *ApJS*, 185, 511
Raiteri, C. M., Villata, M., Tosti, G., et al. 2003, *A&A*, 402, 151
Raiteri, C. M., Villata, M., Ibrahimov, M. A., et al. 2005, *A&A*, 438, 39
Rani, B., Krichbaum, T. P., Lott, B., Fuhrmann, L., & Zensus, J. A. 2013, *Advances in Space Research*, 51, 2358
Rani, B., Gupta, A. C., Strigachev, A., et al. 2010, *MNRAS*, 404, 1992
Romero, G. E., Cellone, S. A., & Combi, J. A. 1999, *A&AS*, 135, 477
Sandrinelli, A., Covino, S., & Treves, A. 2014, *A&A*, 562, A79
Sikora, M., Begelman, M. C., & Rees, M. J. 1994, *ApJ*, 421, 153
Simonetti, J. H., Cordes, J. M., & Heeschen, D. S. 1985, *ApJ*, 296, 46
Smith, P. S., Montiel, E., Rightley, S., et al. 2009, *ArXiv e-prints*, arXiv:0912.3621
Stalin, C. S., Kawabata, K. S., Uemura, M., et al. 2009, *MNRAS*, 399, 1357
Ulrich, M.-H., Maraschi, L., & Urry, C. M. 1997, *ARA&A*, 35, 445
Urry, C. M., & Mushotzky, R. F. 1982, *ApJ*, 253, 38
Urry, C. M., & Padovani, P. 1995, *PASP*, 107, 803
Vestergaard, M. 2004, *ApJ*, 601, 676
Villata, M., Raiteri, C. M., Lanteri, L., Sobrito, G., & Cavallone, M. 1998, *A&AS*, 130, 305
Villata, M., Raiteri, C. M., Kurtanidze, O. M., et al. 2002, *A&A*, 390, 407
Wagner, S. J., & Witzel, A. 1995, *ARA&A*, 33, 163
Wiita, P. J. 1985, *Physics Reports*, 123, 117
Wu, J., Zhou, X., Ma, J., Wu, Z., & Jiang, Z. 2009, in *Astronomical Society of the Pacific Conference Series, Vol. 408, The Starburst-AGN Connection*, ed. W. Wang, Z. Yang, Z. Luo, & Z. Chen, 278
Wu, J., Zhou, X., Peng, B., et al. 2005, *MNRAS*, 361, 155
Xie, G. Z., Liang, E. W., Zhou, S. B., et al. 2002, *MNRAS*, 334, 459
Yuan, Y.-H., Fan, J.-h., Tao, J., et al. 2017, *A&A*, 605, A43
Zdziarski, A. A., & Böttcher, M. 2015, *MNRAS*, 450, L21
Zhang, J., Liang, E.-W., Zhang, S.-N., & Bai, J. M. 2012, *ApJ*, 752, 157
Zhang, J., Xue, Z.-W., He, J.-J., Liang, E.-W., & Zhang, S.-N. 2015, *ApJ*, 807, 51